

# Preparation of Artificial Aggregate Using Waste Concrete Powder And CO<sub>2</sub> Fixed By Microorganisms

Xiao Zhang

Southeast University School of Materials Science and Engineering

Chunxiang Qian (✉ [cxqianseu1@163.com](mailto:cxqianseu1@163.com))

Southeast University <https://orcid.org/0000-0002-7547-5890>

Dengmin Xie

Southeast University School of Materials Science and Engineering

---

## Research Article

**Keywords:** waste concrete, artificial aggregate, microorganism, CO<sub>2</sub> fixation

**Posted Date:** September 1st, 2021

**DOI:** <https://doi.org/10.21203/rs.3.rs-836651/v1>

**License:**   This work is licensed under a Creative Commons Attribution 4.0 International License.

[Read Full License](#)

---

**Version of Record:** A version of this preprint was published at Clean Technologies and Environmental Policy on January 12th, 2022. See the published version at <https://doi.org/10.1007/s10098-021-02258-x>.

# Abstract

High carbon emissions, shortage of natural aggregates and environmental pollution of waste concrete powder (WCP) have become three imperative crises faced by the traditional concrete industry. The waste concrete crushed to prepare aggregates always has poor mechanical properties and low utilization of waste powder. In this paper, WCP was used to prepare artificial aggregates by cold-bonding disk granulation. And a novel approach for strengthening mechanical properties and improving CO<sub>2</sub> sequestration of artificial aggregates was proposed based on using microorganisms. The microorganism enhanced the mechanical properties, porosity and microstructure of artificial aggregates. The apparent density, crushing strength and water absorption of artificial aggregates were increased to 2620 kg/m<sup>3</sup>, 9.1 MPa and 4.8 %, respectively. It showed a denser microstructure because more mineralization products with well crystallization reduced the porosity from 20.98 % to 13.88 %. The CO<sub>2</sub> fixation of artificial aggregates increased from 7.39 wt. % to 16.00 wt. % due to the existence of microorganism. The compressive strength of concrete indicated that artificial aggregate could substitute the nature aggregates partially without affecting its strength, and the better rate should be controlled within 50 wt. %. This method has obvious effect on waste resource utilization and CO<sub>2</sub> emission reduction, displayed good potential for future applications.

## Introduction

Global warming caused by CO<sub>2</sub> emission has gradually become a severe challenge for humankind. Countries and organizations all over the world are contributing to carbon emission reduction (Ma et al., 2020). As the world's largest carbon emitter, China is under enormous pressure to decrease CO<sub>2</sub> emissions (Li et al., 2021). China has committed to achieving carbon dioxide emissions peaking by 2030 and carbon neutralization by 2060 (Zheng et al., 2019). With the development of China's economy, infrastructure and building construction are being at a rapid development stage (Yue et al., 2008). That causes the construction industry has become an essential source of CO<sub>2</sub> emissions (Lu et al., 2020; Peng et al., 2019). As the most significant consumption of concrete in construction, demolition and renovation of old building facilities will produce many waste concretes. The traditional concrete industry urgently needs to reduce waste concrete discharge and carbon emission now and in the future (Bi, 2012; Zhang et al., 2020). Gravel material is not only an indispensable material of concrete but also a non-renewable mineral resource. Excessive mining and consumption demand lead to resource crisis of concrete aggregate. In order to maintain the sustainable development of the construction industry, the technology of using waste concrete to prepare recycled concrete aggregate has been concerned and developed (Dhillon et al.; Emad et al., 2019; Prasittisopin et al., 2017). That can solve the problem of waste concrete disposal, avoid piling up and occupying land to damage the environment, and relieve the pressure of natural aggregate shortage.

However, the traditional aggregate prepared by the crushing and screening process is low strength, high water absorption and poor quality. And the waste powder produced in the crushing process is

continuously discharged, which is used difficultly with low utilization. The new methods should be adopted to prepare high-quality aggregate by all components of waste concrete for fundamentally solving the shortage of natural aggregate resources. In this paper, the artificial concrete aggregate was prepared using the core-shell structure with the waste concrete powder (WCP) as the shell material and the waste concrete aggregate particle (WCAP) as the core, which can make full use of waste concrete powder.

The cold-bonding disk granulation method has been tried to use fly ash (Kockal and Ozturan, 2010; Manikandan and Ramamurthy, 2007; Narattha and Chaipanich, 2018), steel slag powder (Pang et al., 2015), solid waste incineration bottom ash (Tang and Brouwers, 2017; Tang et al., 2017), blast furnace slag (Fca et al., 2015), concrete slurry waste (Hanif and Yusof, 2012; Pei et al.), quarry waste fine powder (Gunning et al., 2009; Job et al., 2019) and other solid waste to prepare aggregates. In preparing aggregate, to improve the basic properties of aggregate, many measures are taken: adding high proportion of binder, strengthening the bonding, excitation intensity through strong alkali solution, and so on. Some technologies' problems are considered: low added value of resource utilization, high cost, and low environmental and ecological benefits. Fortunately, the research shows that minerals containing calcium and magnesium have good carbonation reactivity, which can provide strength by changing the physicochemical properties of raw materials (Moon and Choi, 2019; Olajire, 2013; Zhang et al., 2011). As waste concrete is also a kind of rich-calcium material, it is feasible to strengthen the aggregate by carbonation. Further carbon sequestration can be achieved, which is conducive to reducing the carbon footprint of concrete. In terms of carbon capture technology, microbial enzyme catalysis is undoubtedly the most promising method because of its well-known characteristics of high efficiency and low energy consumption. Microbial mineralization and deposition of calcium carbonate technology is a method to increase the CO<sub>2</sub> fixation rate of minerals through microbial enzyme catalysis, induce calcium ion deposition in the environment, and generate biological calcium carbonate. The application of MIPC in cement-based materials has become an interesting field of research in the present scenario. Previous studies have shown that the deposited microbial calcium carbonate can not only be used to reduce efflorescence, repair concrete cracks (Ashraf, 2016; Huaicheng et al., 2016), but also promote CO<sub>2</sub> absorption and desorption. And the reaction of microbial mineralization is mild, and the product is calcium carbonate, which has excellent environmental friendliness and excellent compatibility with cement-based materials. Therefore, the application of microbial technology to strengthen the performance of artificial aggregate is feasible and predictable.

In this study, firstly, the method of using waste concrete and microbial carbon fixation to prepare man-made aggregate was introduced. The mechanical properties of artificial aggregate were tested, and the porosity and microstructure of artificial aggregate were analyzed by MIP and XCT. Then, the strengthening effect of microorganisms on artificial aggregate and its mechanism are studied. Finally, the carbon fixation effect of artificial aggregate and the performance of concrete prepared by artificial aggregate are evaluated.

# Materials And Methods

## 2.1 Raw materials

### 2.2.1 Waste concrete powder and particle

Waste concrete powder and particle were made by crushing concrete with a jaw crusher, grinding by a centrifugal mill, and sieving. WCP was through a 0.3 mm square hole sieve and WCAP was screened out with a particle size of 2.36 ~ 4.75 mm. The waste concrete was prepared to consist of cement, concrete admixture, water and sand, aggregate by the proportion of 1: 0.45: 0.40: 1.58: 3.04, which were cured more than one year with the compressive strength of 60.5 MPa. The WCP is mainly cement stone and the particle is mainly sand or aggregate. The main minerals are quartz, calcium hydroxide and hydration products of cement such as calcium silicate hydrate, as shown in Fig. 1. And the chemical compositions and particle size distribution of WCP and Portland cement were measured using an energy-dispersive type X-ray fluorescence (XRF) spectrometer (ARL Perform' X-4200, America) and laser particle sizer (Microtrac S3500, America), and the results are shown in Table 1 and Fig. 2, respectively. The major chemical composition is mainly CaO and SiO<sub>2</sub> of waste concrete. The bulk and apparent density of WCP were about 985 kg/m<sup>3</sup> and 2631 kg/m<sup>3</sup>, respectively (according to Chinese standard GB/T 8074 - 2008).

Table 1  
Chemical composition (wt.%) of WCP and cement

	SiO <sub>2</sub>	CaO	Al <sub>2</sub> O <sub>3</sub>	Fe <sub>2</sub> O <sub>3</sub>	SO <sub>3</sub>	K <sub>2</sub> O	Na <sub>2</sub> O	MgO	LOI
WCP	39.85	30.84	6.34	2.03	1.93	1.76	1.13	–	12.18
P-42.5	21.01	63.35	4.23	3.15	2.31	–	–	2.19	3.16

### 2.2.2 Microbial additive

The microorganism used in this paper was *Bacillus mucilaginous*, which could produce carbonic anhydrase. This enzyme could effectively accelerate the hydration and dehydration rate of CO<sub>2</sub>. Under ideal conditions, a single enzyme molecule can catalyze 10<sup>6</sup> CO<sub>2</sub> molecules per second. In our previous work (Qian et al., 2015; Qian et al., 2009), the *Bacillus mucilaginous* with strong adaptability to the alkaline environment was obtained through laboratory microbial domestication and Screening. This bacillus is a facultative gram-positive bacterium with a spindle structure, harmless to the human body and the environment. In this experiment, *bacillus mucilaginous* was inoculated in a sterilized medium solution. The medium was incubated at 25 °C in a shaking incubator at 170 rpm for 72 hours and centrifuged to prepare a concentrated bacterial solution. Then spray dryer was used to transform liquid microbial spores into powdery spores as the microbial additive (MA).

## 2.2 Preparation and curing

In general, cold-bonding disk granulation refers to powder materials under the action of a liquid bridge and capillary tube to form micronuclei, which continuously rotate and grow in the powder layer, and finally form spherical particles of a certain size. However, this study improved the technology by prepare waste concrete sand particles as the core, which is more conducive to formatting and improving performance. The method of cold-bonding disk granulation was slightly different from other methods reported in the literatures, the specific steps are as follows: The WSAP was placed in the granulator in advance with wetting surface. Subsequently, setting the rotation speed at 35 r/min, the powdery materials were continuously fed to the granulator, and an appropriate amount of water was sprayed on the dry powders. The artificial aggregates can be divided into two groups based on the raw material of the shell: As for non-bacterial group(NB), the powder materials included pre-mixed WCP, cement; As for bacterial group (B), MA was added in the powder materials; The mix proportion of core-shell raw materials is listed in Table 2.

Table 2  
Mix proportion of artificial aggregates and curing conditions (g)

	WCP	Cement	WCAP	MA	Water	Curing condition
NB	1000	160	100	0	187	(a)
B	1000	160	100	10	187	(a)
NB-C	1000	160	100	0	187	(b)
B-C	1000	160	100	10	187	(b)

After granulation, all artificial aggregates were placed in the standard curing room for 24hours. And the relative humidity was more than 90% RH. The temperature was  $20\pm 2^{\circ}\text{C}$ ,  $\text{CO}_2$  concentration was about 0.03%. The Initial curing time can ensure the germination and growth of microorganisms and get a little strength due to the hydration of cement. Then two curing systems were designed to investigate the properties of artificial aggregates under different  $\text{CO}_2$  concentrations at standard atmospheric pressure. (a) Curing in the room environment condition (RC): the  $\text{CO}_2$  volume fraction was about 0.03%, the temperature was  $20\pm 2^{\circ}\text{C}$ , and relative humidity was  $70\pm 5\%$ ; (b) Cuing in carbonation box: the  $\text{CO}_2$  volume fraction was  $95\pm 1\%$ , the temperature was  $20\pm 2^{\circ}\text{C}$ , and relative humidity was  $70\pm 5\%$ , as shown in Table 2.

For example, Fig. 3 shows the preparation process and raw material of artificial aggregate as B-C group. The first step, waste concrete was crushed, ground, and screened to waste concrete powder (WCP, diameter less than 0.3mm) and waste concrete aggregate particles (WCAP, diameter within 2.36~4.75 mm); the Second step, WCAP was used as core and cement, MC, WCP as shell material and for cold-bonding disk granulation; Third, curing in the carbonated box.

## 2.3 Methods

### 2.3.1 Mechanical properties

For studying the effect of microorganisms on the improvement of artificial aggregate after different curing times in two curing conditions, the apparent density, 24-hours water absorption and crushing strength are investigated to reflect the mechanical properties of artificial aggregates with curing 30 hours. The apparent density and 24 h water absorption were measured following Chinese standard GB/T14685-2011 and GB/B 17431.2–2010. A California bearing ratio tester was used to determine the crushing strength value of the prepared artificial aggregates. Before the test, a vernier caliper was used to test the diameter of aggregates in two vertical directions, and the average value was taken as the result. Placed the aggregates between two parallel plates, kept the stiffener's loading rate at 0.5 mm/min, recorded the maximum pressure value when the aggregates were broken, and took 50 aggregates in each group. The principles of testing are shown in Fig. 4. According to the literatures (Arslan and Baykal, 2006; Li et al., 2000), the strength of aggregates can be measured by testing the crushing strength of a single aggregate in accordance with the following Eq. (1):

$$\sigma = \frac{2.8P}{\pi d^2} \text{ Eq. (1)}$$

where,  $\sigma$  is crushing strength (MPa),  $P$  is failure load (N),  $d$  is diameter of artificial aggregates (mm).

## 2.3.2 Micro-morphology and structure of aggregate shell

Furthermore, in order to study the effect of microorganism on micro-morphology of artificial aggregate, the NB and NB-C groups after curing 24 hours were broken, and the shell parts were taken to test. Small particles the size of 1 ~ 2 mm dried for 3 days drying oven and subjected to a gold coating process to ensure good electrical conductivity. Then the surface micro-morphologies of the samples were observed under a scanning electron microscopy with energy dispersive X-ray spectroscopy (SEM-EDX, Sirion, Netherlands). Mercury Intrusion Porosimetry (MIP, Auto pore IV 9510, Micromeritics USA) was adopted to test the porosity of artificial aggregate. Specially, the samples need to be dried in a vacuum drying oven at 60°C for 7 days to meet the vacuum requirements before testing.

## 2.3.3 Microstructure of artificial aggregate

For observation of the microstructure and composition of artificial aggregate with and without microorganism, the NB, B, NB-C and B-C artificial aggregate specimen with curing 24 hours were adopted. X-ray computed tomography (X-CT, Y.CT precision, Germany) were used to analyze the 3D pore structure of whole artificial aggregates, respectively.

## 2.3.4 CO<sub>2</sub> fixation of artificial aggregate

CO<sub>2</sub> weight and CO<sub>2</sub> fixation of artificial aggregates after curing 24 hours were quantified by thermogravimetric analysis (TG, STA 449 F3, Germany) as per Eq. (2) (3) respectively (Jiang and Ling, 2020). The aggregates particles with the sizes of 16 ± 2 mm were chosen, and about 10 mg of the homogeneously ground sample was weighed and heated from 25°C to 950°C at a heating rate of 10°C/min in a nitrogen atmosphere.

$$\Delta\text{CO}_2 \text{ (wt.\%)} = (W_{600} - W_{800}) \times 100 \text{ Eq. (2)}$$

$$\text{CO}_2 \text{ fixation (wt.\%)} = \frac{\Delta\text{CO}_2 \text{ (wt.\%)}_{\text{after}} - \Delta\text{CO}_2 \text{ (wt.\%)}_{\text{before}}}{100 - \Delta\text{CO}_2 \text{ (wt.\%)}_{\text{after}}} \times 100 \text{ Eq. (3)}$$

Where  $W_{600}$  and  $W_{800}$  represent the Mass loss of the aggregate at 520°C and 780 °C, respectively. And the  $\Delta\text{CO}_2$  (wt. %) after means the  $\Delta\text{CO}_2$  (wt. %) value of artificial aggregate after curing stage, the  $\Delta\text{CO}_2$  (wt. %) before means the  $\Delta\text{CO}_2$  (wt. %) value of fresh-formed artificial aggregate without curing stage.

## 2.3.5 Compressive strength of concrete

The nature aggregate and artificial aggregate of the B-C group were used to prepare the concrete. The compressive strength of the samples with the size of 100mm×100 mm×100 mm was based on the Chinese standard GB/T 50081 – 2019. Every group with three samples was calculate based on the following formula Eq. (4), and the result was accurate to 0.1 MPa.

$$f_{cc} = \alpha \frac{F}{A} \text{ Eq. (4)}$$

Where the  $f_{cc}$  refers to the compressive strength of concrete samples (Mpa), the  $F$  refers to the failure load of samples (N), the  $A$  refers to the loaded area of samples ( $\text{mm}^2$ ), the  $\alpha$  refers to Dimension conversion factor (0.95).

## Results And Discussion

### 3.1 Mechanical properties of artificial aggregate

The evolution of apparent density, crushing strength, and water absorption of artificial aggregates with different time are shown in Fig. 5. It can be clearly observed that with the presence of microorganisms, the mechanical properties of artificial aggregates (B or B-C group) are better than that of NB or NB-C. As for the group of NB and B (In curing (b) condition), the mechanical properties have a little change with the increase of curing time. As for the group of NB-C and B-C, the value of apparent density and crushing strength gradually increase and then keep stable.

As for NB group, the mechanical properties are improved because during the hardening process of aggregates, the cement hydration products (mainly calcium hydroxide (CH) and calcium silicate hydrates (C-S-H)) were gradually produced (Bye, 1999), which improved the performance of the aggregates. And with adding the microorganisms, the mechanical properties improvement effect is not apparent because of low  $\text{CO}_2$  concentrate. When cured in the  $\text{CO}_2$  concentration above 95% ((b) condition), the mechanical properties of artificial aggregates were improved a lot. For example, after curing for 24 h, the apparent density of the NB-C group was  $2520 \text{ kg/m}^3$ , crushing index was 4.4 MPa, and water absorption was 9.7%, while NB of those were  $2400 \text{ kg/m}^3$ , 2.3 MPa, and 11.5% respectively, which was consistent with other studies (Jiang and Ling, 2020). The above phenomenon could be explained by the reaction of calcium

hydroxide from WCP/cement hydration and carbon dioxide then produced calcium carbonate with higher elastic modulus. More carbonated productions also compacted the microstructure (Ashraf, 2016; Zhan et al., 2016). Furthermore, the microorganisms show a huge promotion effect in high CO<sub>2</sub> concentration. Compared with the NB-C group, the apparent density of aggregates in B-C was 2620 kg/m<sup>3</sup> (an increase of 4%), crushing strength was 9.1 MPa (an increase of 106.8%), and water absorption was 4.8% (decrease of 50.5%) after cured 24 hours. Obviously, the presence of microorganisms accelerated the carbonation process, and more carbonated productions change the microstructure of artificial aggregates, which made the strengthening effect more conspicuous.

## 3.2 3D pore structure of artificial aggregate

X-CT is reviewed as the most advanced non-destructive test methodologies for the evaluation of cement-based materials at the micro-structural level (Lu et al., 2007; Prasad, 2020). The distribution of pores and the connectivity of the pores with respect to their location can be visualized by reconstructing three/two-dimensional sections. The pore structure of 4-types artificial aggregates was investigated by X-ray computed tomography to explore the effect of mineralization by microorganisms. Figure 6 shows the X-CT 3D reconstruction of artificial aggregates, from blue to red, the defect volume gradually increased. For the NB group, the whole structure showed many properties, with a maximum defect volume of 1.84mm<sup>3</sup>. After curing 95% CO<sub>2</sub> condition (curing (b) condition), it was worth noting that the porosity of NB-C showed an apparently gradient porosity structure. From the edge to the center of the pellet, the colored area gradually became denser, which indicated that the porosity gradually raised. Because the CO<sub>2</sub> concentration at the edge was higher than inside. With the increased depth, the concentration of carbon dioxide gradually reduced.

Furthermore, the products generated at the edge hindered the transmission of carbon dioxide, resulting in a slower rate and lower degree of internal carbonation reaction. However, the presence of microorganisms in artificial aggregate increased the CO<sub>2</sub> concentration inside. For the B group, the blue-colored area was sparse than the NB group because the microorganism uniformly distributed in the whole aggregate in advance accelerated the capture of CO<sub>2</sub>. In high CO<sub>2</sub> concretion, the microorganism increased the carbonated depth. For the B-C group, gradient structure in a shell of artificial aggregate was not detected, and deeper distances from the surface show less pore. That means microorganisms could make the carbonation reaction more complete and the aggregate structure more uniform.

In X-CT, quantitative analysis on void content and size of pores was determined by obtaining the two-dimensional images as the result of the various intensities with correlation to the material's density (Seibert and Boone, 2005; Wei et al., 2011). Figure 7 shows the 2D of artificial aggregates, and the black spots were identified as the voids in the cementitious matrix. It can be found that the B-C are denser than other groups, also reflect the improvement of microorganisms on the microstructure of artificial aggregate. Additionally,

## 3.3 Porosity of artificial aggregate shell

In order to analyze the improvement of microorganisms on porosity of artificial aggregate, the specimens of shell structure were tested by MIP. The porosity content is obtained as the total volume of the mercury intruded into the aggregates pellet to the total volume of the sample was used to accurately analyze the micropores of aggregates ranging from 3 nm to 5000 nm. The integral curves and differential curves of the pore size distribution of artificial aggregates with and without bacteria under different curing conditions are shown in Fig. 8. Formerly, the calculation of the results data is listed in Table 3. It can be found that the porosities of NB and B group are similar, which are 30.45 and 29.78 respectively, indicating that the addition of microorganism would not improve porosity. But the average pore diameter and most probable aperture decreased because mineralization productions originated by microorganisms and WCP/cement filled the pore. However, after curing in CO<sub>2</sub> with a concentration above 95%, it was worth mentioning that the porosity of the B-C group had the most significant decline, which was only 13.88%. Meanwhile, the average pore diameter and most probable diameter also decrease. That can be concluded that the microorganism can significantly modify the micro-pore structure of artificial aggregates. It should be specially pointed out that the most aperture of B was only 9.02 nm, which was classified as harmless pore (ZhongWei, 1979), which was greatly beneficial for aggregates to resist the invasion of foreign harmful substances.

Table 3  
Pore structure characteristics of four types of artificial aggregate

Samples	Porosity/%	Average pore diameter/nm	Most probable aperture/nm
NB	30.45	208.45	793.12
B	29.78	186.65	609.53
NB-C	20.98	41.25	348.90
B-C	13.88	12.44	9.02

### 3.4 Micro-morphology of carbonated and mineralized products in shell

The artificial aggregates after curing 95% concentration CO<sub>2</sub> condition showed better mechanical and denser microstructure. Therefore, the shell parts of artificial aggregates without and with microorganisms (NB-C and B-C groups) were adopted to study the effect of microorganisms by SEM. Figure 9 and Fig. 10 showed the SEM images of micro-morphology of carbonated and mineralized products in the shell, respectively. There were obvious crystal depositions on the surface of the artificial aggregates. From the analysis of the EDS (Fig. 9 (d)), the major elements NB-C are C, Ca, and O, which proves that carbonated products are calcium carbonate. The other products may be calcium silicate hydrate because the detection of tiny Si elements. The crystal morphology of products deposited of NB-C shows mainly ellipsoidal and massive, and relatively sparse. Figure 10(d) also proved the mineralized products are calcium carbonated. Differently, the crystal on the surface shown in Fig. 10(c) was mainly irregular with

crisscross growth and denser, which was just the favorable evidence of microbial promoting calcium carbonate deposition.

### 3.5 Analyze the mechanical of artificial aggregate concrete

The artificial aggregate was replaced by 10%, 30%, 50%, 70% and 100% of natural aggregate to prepare concrete. The apparent density surface of nature and artificial aggregate is 2730 kg/ m<sup>3</sup>, 2600 kg/m<sup>3</sup>, and the water absorption of 0.7% and 3.0%. There is a certain gap in the apparent density of both aggregates. The specific mix proportion was calculated based on the volume method. The proportion of various materials with 1 m<sup>3</sup> are shown in Table 4.

Table 4  
Mix proportion of concrete (kg)

Code	Replace ratio/%	Cement	Water	Sand	Nature aggregate	Artificial aggregate
NC	0	360	180	640	1114	0
AC-10	10	360	180	640	1003	107
AC-30	30	360	180	640	780	321
AC-50	50	360	180	640	557	535
AC-70	70	360	180	640	334	749
A-100	100	360	180	640	0	1070

Figure 11 shows the strength of natural aggregate concrete (NC) and artificial aggregate concrete (AC) with a different replacement under curing seven days and 28 days. The compressive strength of NC or AC shows a similar strength-development trend. The compressive strength increases with age, and the strength with curing 7-day can reach above 70% of the 28-day strength. When the replacement rate of artificial aggregate is less than 30%, the compressive strength of AC has little change and slightly increases compared with that of NC. However, when the replacement rate reaches 50%, the compressive strength of concrete reaches NC concrete. When more than 50%, the compressive strengths decrease sharply, with the maximum reduction of 22.4% at AC-100 group. The low replacement rate has little effect on the concrete strength because the water absorption rate of aggregate is higher than that of natural aggregate. Increasing the replacement material within a certain range reduces the effective water-cement ratio of concrete, which reduces the porosity. And in the long-term curing, the moisture absorbed by artificial aggregate will be released to the matrix gradually with the hydration process of concrete cement, which is conducive to the development of strength. In addition, part of the cement slurry is easily attached to the surface micropores of coarse aggregate, making the mosaic structure between aggregate and matrix. However, there is no doubt that the compressive strength of concrete mainly depends on the coarse aggregate. The high replacement rate will inevitably lead to a significant reduction in the strength of concrete due to the low strength of artificial aggregate. Therefore, the artificial aggregate prepared in this study can replace the natural aggregate in a certain proportion to prepare concrete, and the maximum content should be controlled within 50%.

### 3.6 CO<sub>2</sub> fixation of artificial aggregate

The thermogravimetric (TG) and differential thermogravimetric (DTG) curves of artificial aggregates are plotted in Fig. 12. The peaks observed in DTG curve (600 ~ 800°C) were mainly denoted the decomposition of calcium carbonates (Shah et al., 2018). According to Eqs. (2) and (3), CO<sub>2</sub> change ( $\Delta\text{CO}_2$ ) and fixation of artificial aggregate are listed in Table 5. It should be specially pointed out that CO<sub>2</sub> fixation in the table refers to the result after deducting the CO<sub>2</sub> content of WCP itself (2.34 wt. % detected). The CO<sub>2</sub> content in WCP was derived from the absorption of CO<sub>2</sub> in the atmosphere by the waste concrete matrix. The CO<sub>2</sub> fixation of NB and B groups were similar and less than 1 wt. % due to the low CO<sub>2</sub> concentration, indicating that the CO<sub>2</sub> fixation ability of is weak. However, under 95% CO<sub>2</sub> concentration, the CO<sub>2</sub> fixation increase a lot. And with the presence of microorganisms, the CO<sub>2</sub> fixation of B-C increase from 7.39 wt. % to 16.00 wt. %, illustrating that microorganism further enhanced the carbon fixation capacity of artificial aggregates under high CO<sub>2</sub> concentration. The artificial aggregates mixed with bacteria show great carbon fixation potential. The production of the per-ton artificial aggregate product can fix 160 kg CO<sub>2</sub>, which has remarkable economic and social significance for the construction industry to reduce carbon footprint.

Table 5  
 $\Delta\text{CO}_2$  and CO<sub>2</sub> fixation of artificial aggregates  
(wt. %)

	NB	B	NB-C	B-C
$\Delta\text{CO}_2$	2.52	2.98	9.06	16.81
CO <sub>2</sub> fixation	0.19	0.66	7.39	16.00

### 3.7 Economic and Environmental analysis of artificial aggregate

The production cost of artificial aggregate mainly includes raw material and process cost. The WCP and WACP are parts of waste concrete, by-products produced in the process of crushing and screening of constructions. Therefore, the utilization of solid waste can get government support and government support and preferential policies. According to the relevant tax law of China, the nature aggregate of sand and stone is subject to resource tax of 1% ~ 5%. In addition, 10% of the goods value-added tax is required for production and sales. However, the artificial aggregate produced with construction waste shall be exempted for the sale of self-produced construction aggregates. As a result, the cost and profit are considerable.

The CO<sub>2</sub> fixation content of per ton artificial aggregate with adding microorganisms can reach 154.3 kg, calculating based on the CO<sub>2</sub> fixation of shell parts with 16.0%. The annual output of waste concrete in China is about 1.5 billion tons in 2020. The WCP reach 10% ~ 20%, above 150 million tons in 2020. If all

of them are used to prepare artificial aggregate, about 200 million tons of artificial aggregate can be produced, and 31 million tons of CO<sub>2</sub> can be fixed. According to the carbon emission report of “carbonate dioxide emission report of China building materials industry (2020)”, the CO<sub>2</sub> emission of building materials industry in 2020 is 1.48 billion tons. The rate of reduction CO<sub>2</sub> by produced artificial aggregate can reach 2.09%, which is better for the construction industrial carbon reduction. In the process of production artificial aggregate, it can not only use the waste concrete but also fix CO<sub>2</sub> from cement production process. This method can effectively realize the utilization of waste concrete resources, reduce the exploitation of natural aggregate, and reduce concrete carbon emissions in the whole life cycle, which provided significant economic and environmental benefits.

## Conclusion

In this paper, the artificial aggregate with core-shell structure was prepared by granulation of waste concrete materials, and CO<sub>2</sub> was fixed by microorganisms in the shell to strengthen the aggregate. The influences of microorganisms on the basic properties and microstructure of artificial aggregate were studied. The mechanism of improving mechanical properties and microstructures of artificial aggregate by microorganism was analyzed. The compressive strength of concrete prepared by partial substitution of artificial aggregate was studied. Finally, the economic and ecological benefits of artificial aggregate were analyzed. The specific conclusions are as follows:

- (1) Artificial aggregates (NB-C group) have excellent mechanical properties: the sample's apparent density, crushing strength and water absorption of the samples after curing (b) situation 24 hours were 2620 kg/m<sup>3</sup>, 9.1 MPa and 4.8%, respectively.
- (2) The presence of microorganisms promotes the carbonization of WCP and calcium silicate hydrate in artificial aggregates. More mineralization production dense the structure and reduce the porosity. The calcite crystals with more compact and complete crystal growth were formed in the shell part due to the addition of microorganisms. The porosity of artificial aggregate decreased from 20.98–13.88%, the CO<sub>2</sub> fixation decreased from 7.39 wt. % to 16.00 wt. %.
- (3) The artificial aggregates can replace the natural aggregate in a certain proportion to prepare concrete, when the replacement rate less than 50%, the mechanical properties of concrete have no adverse change.
- (4) The artificial aggregate prepared by microbial CO<sub>2</sub> fixation can make full use of waste concrete powder and reduce the exploitation of natural aggregate. It also can be used for industrial CO<sub>2</sub> fixation and reduce the carbon footprint of the life cycle concrete. The technology of microbial mineralization has mild reaction conditions and a friendly environment. Artificial aggregate products have good market prospects and obvious economic, social and environmental benefits.

## Declarations

# Acknowledgments

The authors appreciate the financial support from the National Nature Science Foundation of China (Grant No. 51738003).

# Disclaimers

The authors declared that they have no conflicts of interest in this work.

# Author statement

In this paper, Xiao Zhang: assist in the preparation samples and test, analysed data, revised and modified the manuscript. Chunxiang Qian: methodology, funding acquisition, conceived the central idea and directed the experiments of this study, writing-review. Dengmin Xie: investigation, conceptualization, methodology, experiments, data curation, analyzed data, writing-original draft.

# References

1. Arslan H, Baykal G (2006) Analyzing the crushing of granular materials by sound analysis technique. *J Test Eval* 34(6):464–470
2. Ashraf W (2016) Carbonation of cement-based materials: Challenges and opportunities. *Construction Building Materials* 120(sep.1):558–570
3. Bi XS (2012) The Review and Prospect Based on Recycled Concrete. *Applied Mechanics Materials* 174–177:970–973
4. Bye GC (1999) 8. The nature of hardened cement paste. Thomas Telford
5. Dhillon AS, Dewangan A, Gupta D, The significance of Strength of Recycle Concrete Aggregate
6. Emad M, Soliman NM, Bashandy AA (2019) 2019- IJCIET- Recycle Aggregate High-strength Concrete- [Emad M.-Soliman N. - Bashandy A.]. *International Journal of Civil Engineering and Technology* 10(9), 128–146
7. Fca B, Fma B, Rca B (2015) Recycling of MSWI fly ash by means of cementitious double step cold bonding pelletization: Technological assessment for the production of lightweight artificial aggregates. *J Hazard Mater* 299:181–191
8. Gunning PJ, Hills CD, Carey PJ (2009) Production of lightweight aggregate from industrial waste and carbon dioxide. *Waste Manag* 29(10):2722–2728
9. Hanif M, Yusof (2012) Mechanical behaviour of concrete made with coarse recycle concrete of aggregates. Universiti Malaysia Perlis
10. Huaicheng C, Chunxiang, Qian, Haoliang, Huang (2016) Self-healing cementitious materials based on bacteria and nutrients immobilized respectively. *Construction & Building Materials*

11. Jiang Y, Ling TC (2020) Production of artificial aggregates from steel-making slag: Influences of accelerated carbonation during granulation and/or post-curing - ScienceDirect. *Journal of CO<sub>2</sub> Utilization* 36:135–144
12. Job T, Harilal B (2019) Sustainability evaluation of cold-bonded aggregates made from waste materials. *Journal of Cleaner Production*
13. Kockal NU, Ozturan T (2010) Effects of lightweight fly ash aggregate properties on the behavior of lightweight concretes. *J Hazard Mater* 179(1–3):954–965
14. Li S, Wu Q, Zheng Y, Sun Q (2021) Study on the Spatial Association and Influencing Factors of Carbon Emissions from the Chinese Construction Industry
15. Li Y, Wu D, Zhang J, Liu C, Shi Y (2000) Measurement and statistics of single pellet mechanical strength of differently shaped catalysts. *Powder Technol* 113(1–2):176–184
16. Lu S, Landis E, Keane N, D., T (2007) X-ray microtomographic studies of pore structure and permeability in Portland cement concrete. *Mater Struct* 39(6):611–620
17. Lu N, Feng S, Liu Z, Wang W, Lu H, Wang M (2020) The Determinants of Carbon Emissions in the Chinese Construction Industry: A Spatial Analysis. *Sustainability* 12(4)
18. Ma CH, Wang M, Wang Z, Gao M, Wang JX (2020) Recent progress on thin film composite membranes for CO<sub>2</sub> separation. *Journal of Co<sub>2</sub> Utilization* 42:22
19. Manikandan R, Ramamurthy K (2007) Influence of fineness of fly ash on the aggregate pelletization process. *Cem Concr Compos* 29(6):456–464
20. Moon EJ, Choi YC (2019) Carbon dioxide fixation via accelerated carbonation of cement-based materials: Potential for construction materials applications. *Constr Build Mater* 199:676–687
21. Narattha C, Chaipanich A (2018) Phase characterizations, physical properties and strength of environment-friendly cold-bonded fly ash lightweight aggregates. *J Clean Prod* 171(pt.2):1094–1100
22. Olajire AA (2013) A review of mineral carbonation technology in sequestration of CO<sub>2</sub>. *J Petrol Sci Eng* 109:364–392
23. Pang B, Zhou Z, Xu H (2015) Utilization of carbonated and granulated steel slag aggregate in concrete. *Construction Building Materials* 84(jun.1):454–467
24. Pei T, Dongxing, Xuan, Hiu, Wun, Cheng C, Poon S, Use of CO<sub>2</sub> curing to enhance the properties of cold bonded lightweight aggregates (CBLAs) produced with concrete slurry waste (CSW) and fine incineration bottom ash (IBA) - ScienceDirect. *Journal of hazardous materials* 381, 120951–120951
25. Peng Wu, Yongze, Song, Jianbo, Zhu, Ruidong C (2019) Analyzing the influence factors of the carbon emissions from China's building and construction industry from 2000 to 2015. *Journal of Cleaner Production*
26. Prasad C (2020) High-efficiency techniques and micro-structural parameters to evaluate concrete self-healing using X-ray tomography and Mercury. A review, *Intrusion Porosimetry*
27. Prasittisopin L, Chaiyapoom P, Thongyothee C, Snguanyat C (2017) Using Recycle Concrete Aggregate Coating Agent for Improving Concrete Microstructure and Hardened Characteristics,

Holistic Innovative Solutions for an Efficient Recycling and Recovery of Valuable Raw Materials from Complex Construction and Demolition Waste (HISER)

28. Qian C, Chen H, Ren L, Luo M (2015) Self-healing of Early Age Cracks in Cement-based Materials by Mineralization of Carbonic Anhydrase Microorganism. *Front. Microbiol.* 6(314)
29. Qian C, Wang J, Wang R, Cheng L (2009) Corrosion protection of cement-based building materials by surface deposition of  $\text{CaCO}_3$  by *Bacillus pasteurii*. *Materials Science Engineering C-Biomimetic Supramolecular Systems* 29(4):1273–1280
30. Seibert JA, Boone JM (2005) X-ray imaging physics for nuclear medicine technologists. Part 2: X-ray interactions and image formation. *J Nucl Med Technol* 33(1):3–18
31. Shah V, Scrivener K, Bhattacharjee B, Bishnoi S (2018) Changes in microstructure characteristics of cement paste on carbonation. *Cem Concr Res* 109:184–197
32. Tang P, Brouwers H (2017) Integral recycling of municipal solid waste incineration (MSWI) bottom ash fines (0–2 mm) and industrial powder wastes by cold-bonding pelletization. *Waste Management* 62(APR.), 125–138
33. Tang P, Florea M, Brouwers H (2017) Employing cold bonded pelletization to produce lightweight aggregates from incineration fine bottom ash. *Journal of Cleaner Production* 165
34. Wei Q, Leblon B, Rocque AL (2011) On the use of X-ray computed tomography for determining wood properties: a review. *Can J For Res* 227(41):2120–2140
35. Yue H, Bird RN, Heidrich O (2008) A review of the use of recycled solid waste materials in asphalt pavements. *Resources Conservation Recycling* 52(1):58–73
36. Zhan BJ, Xuan DX, Poon CS, Shi CJ (2016) Effect of curing parameters on  $\text{CO}_2$  curing of concrete blocks containing recycled aggregates. *Cem Concr Compos* 71:122–130
37. Zhang J, Ding L, Li F, Peng J (2020) Recycled Aggregates from Construction and Demolition Wastes as Alternative Filling Materials for Highway Subgrades in China. *J Clean Prod* 255:120223
38. Zhang T, Yu Q, Wei J, Li J, Zhang P (2011) Preparation of high performance blended cements and reclamation of iron concentrate from basic oxygen furnace steel slag. *Resources Conservation Recycling* 56(1):48–55
39. Zheng J, Mi Z, Coffman D, Shan Y, Wang S (2019) The Slowdown in China's Carbon Emissions Growth in the New Phase of Economic Development. *One Earth* 1(2):240–253
40. ZhongWei W (1979) An approach to the recent trends of concrete science and technology. *Journal of the Chinese Ceramic Society* 7(3):82–90

## Figures

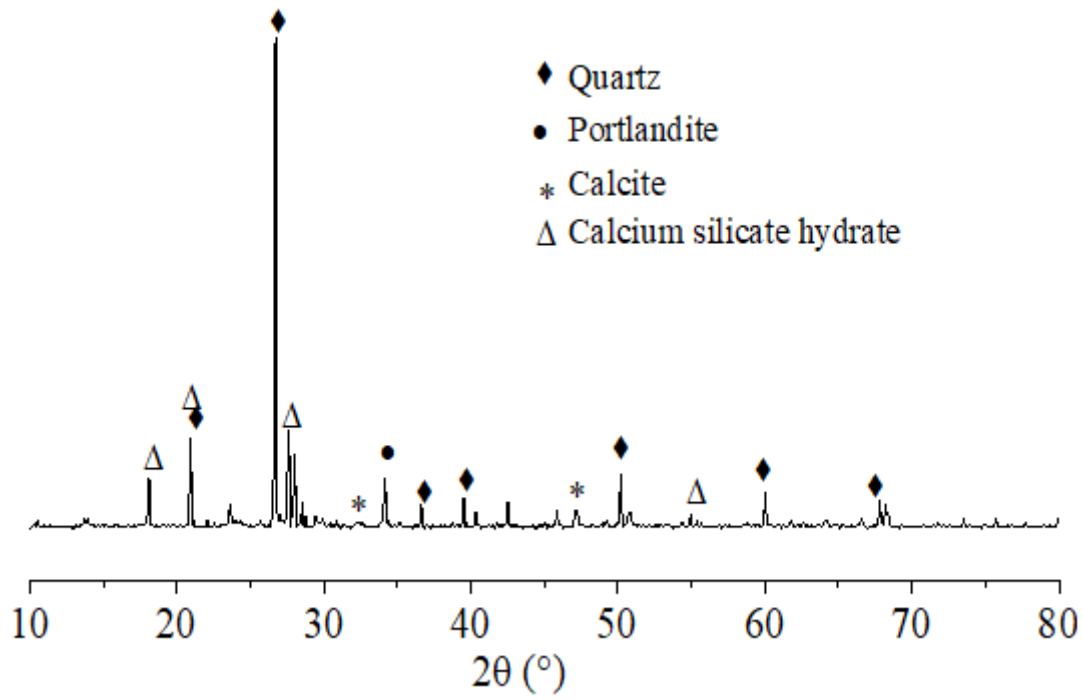


Figure 1

Particle size distribution of WCP and cement

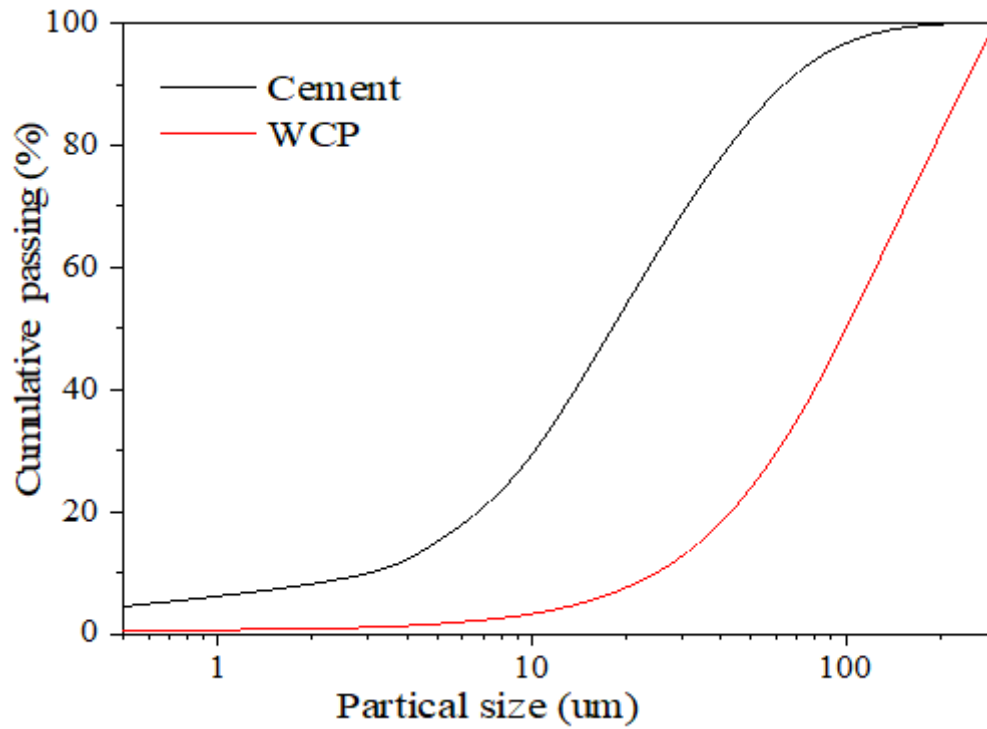


Figure 2

XRD patterns of WCP

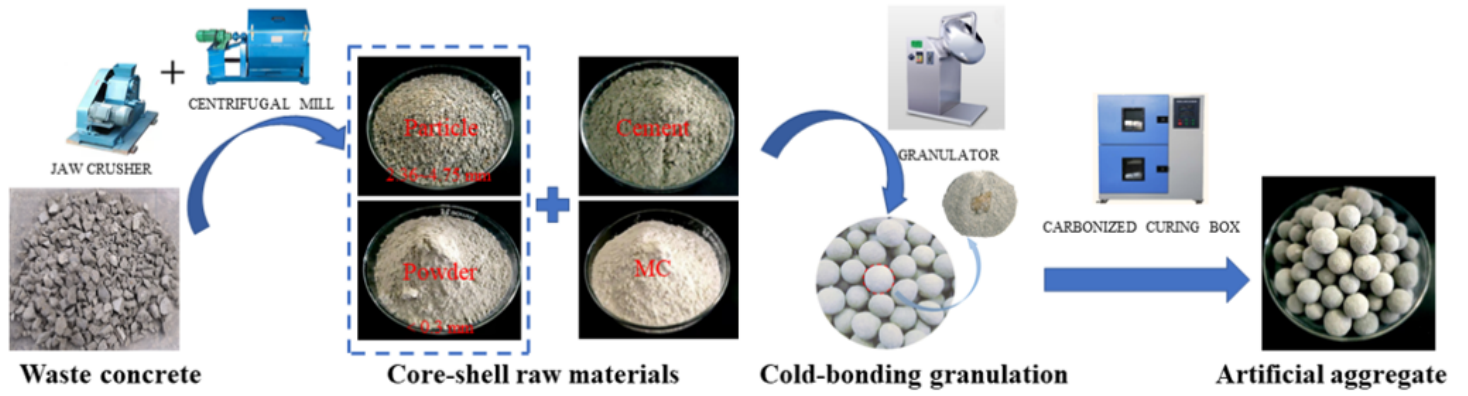


Figure 3

The preparation process and raw material of artificial aggregate

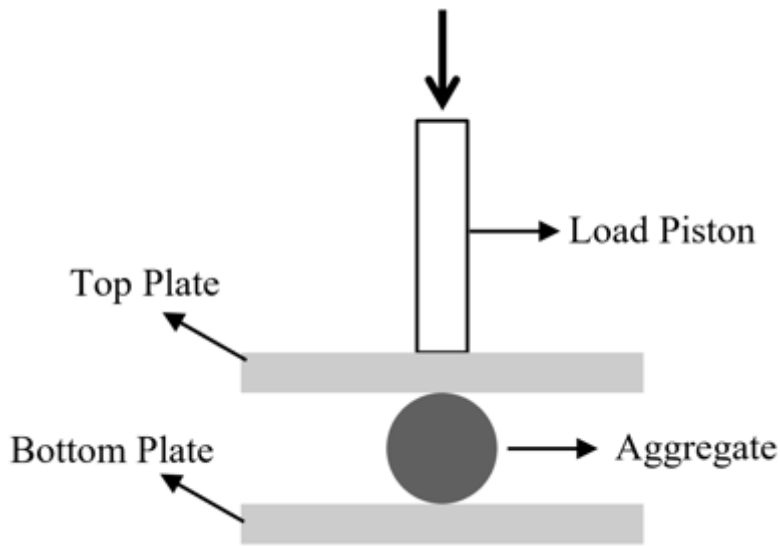
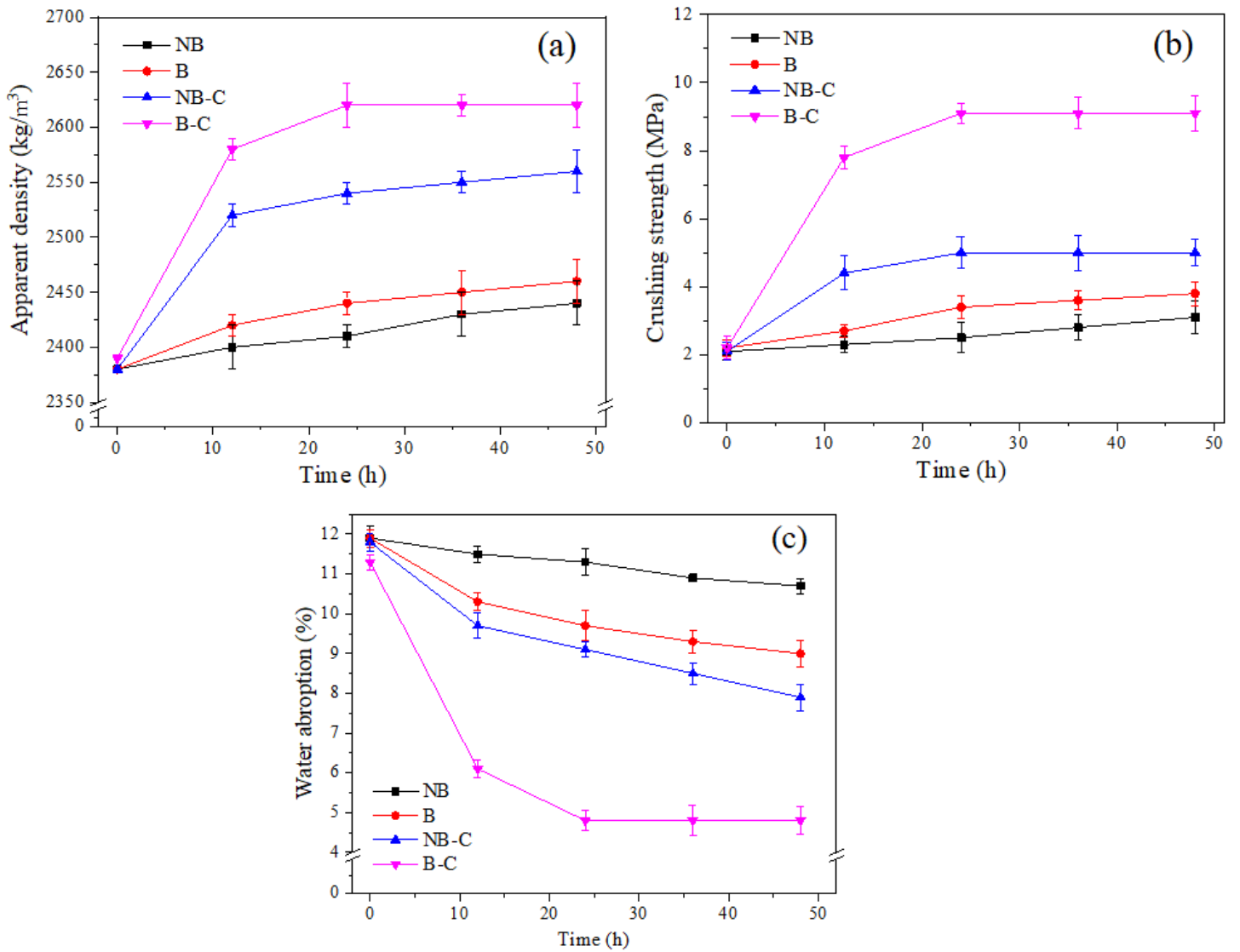


Figure 4

Schematic diagram of artificial aggregates strength measurement



**Figure 5**

The properties of artificial aggregates with curing different time: (a) Apparent density, (b) Crushing strength, (c) Water absorption

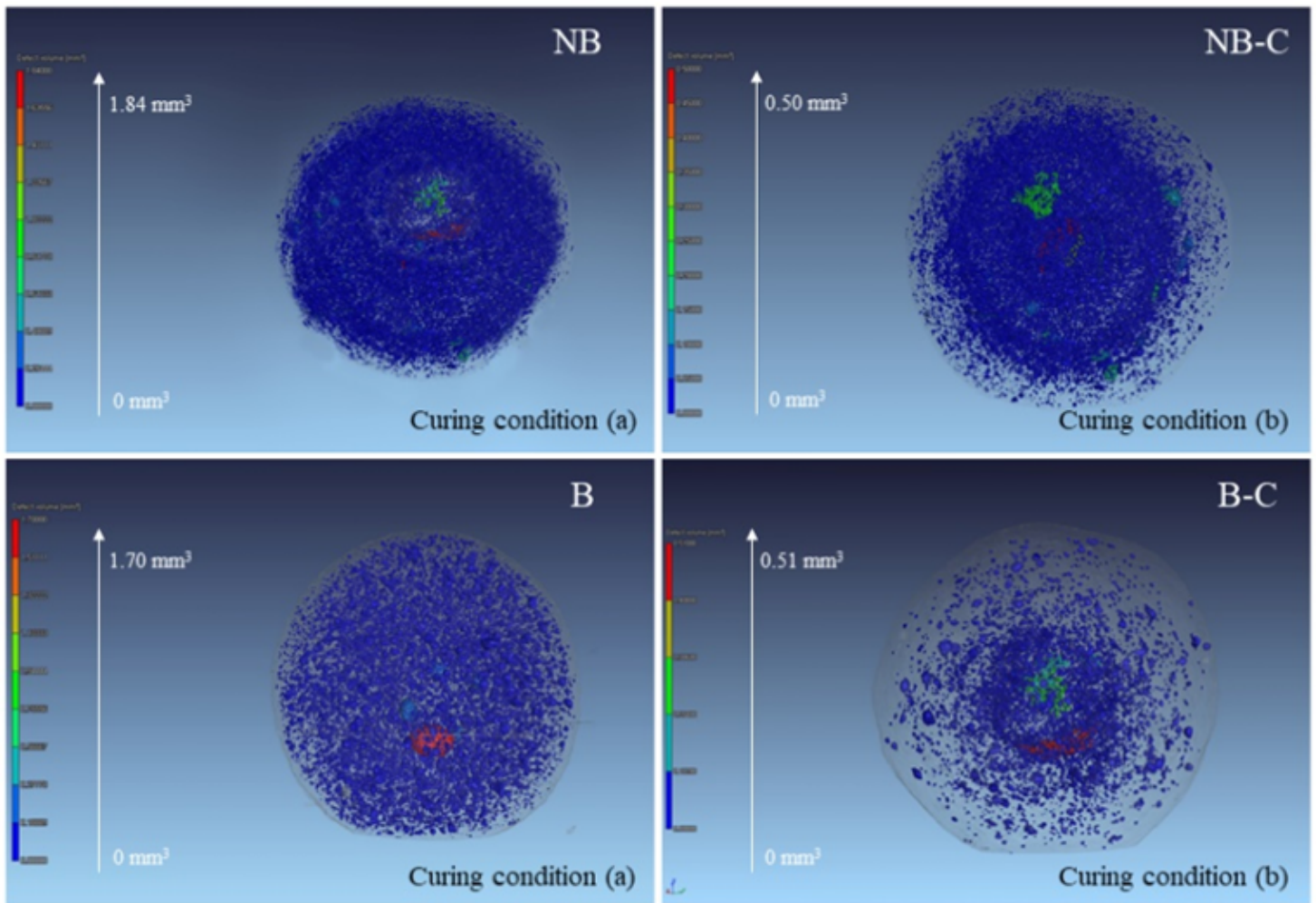


**Figure 6**

3D pore structure evolution of the artificial aggregates with different curing condition

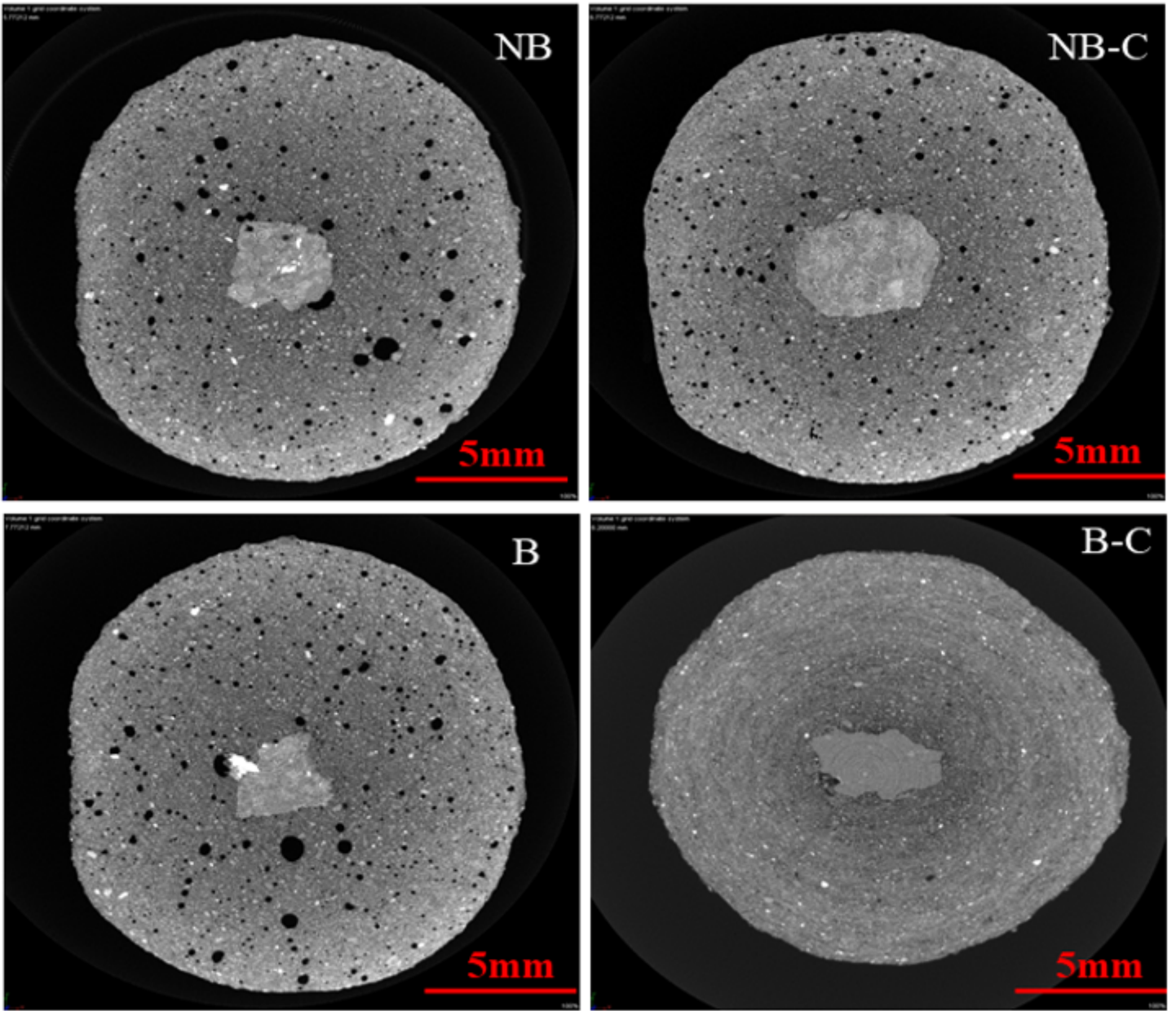


Figure 7

X-CT of the two-dimensional section of artificial aggregates center

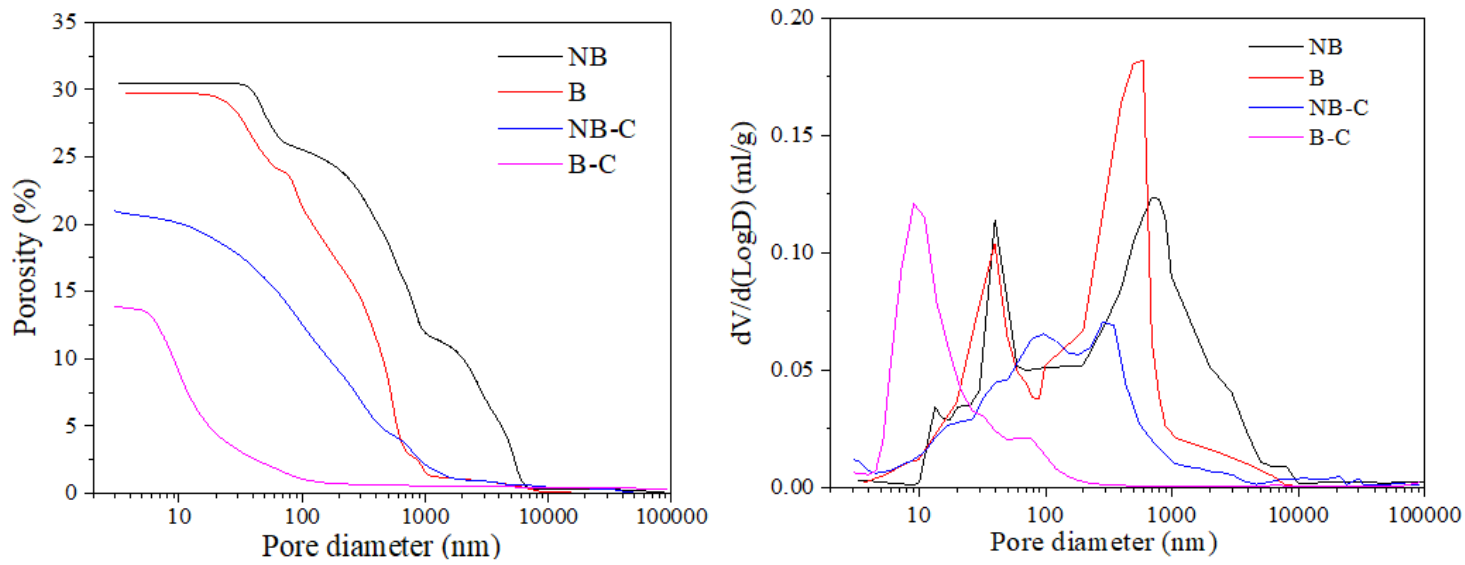
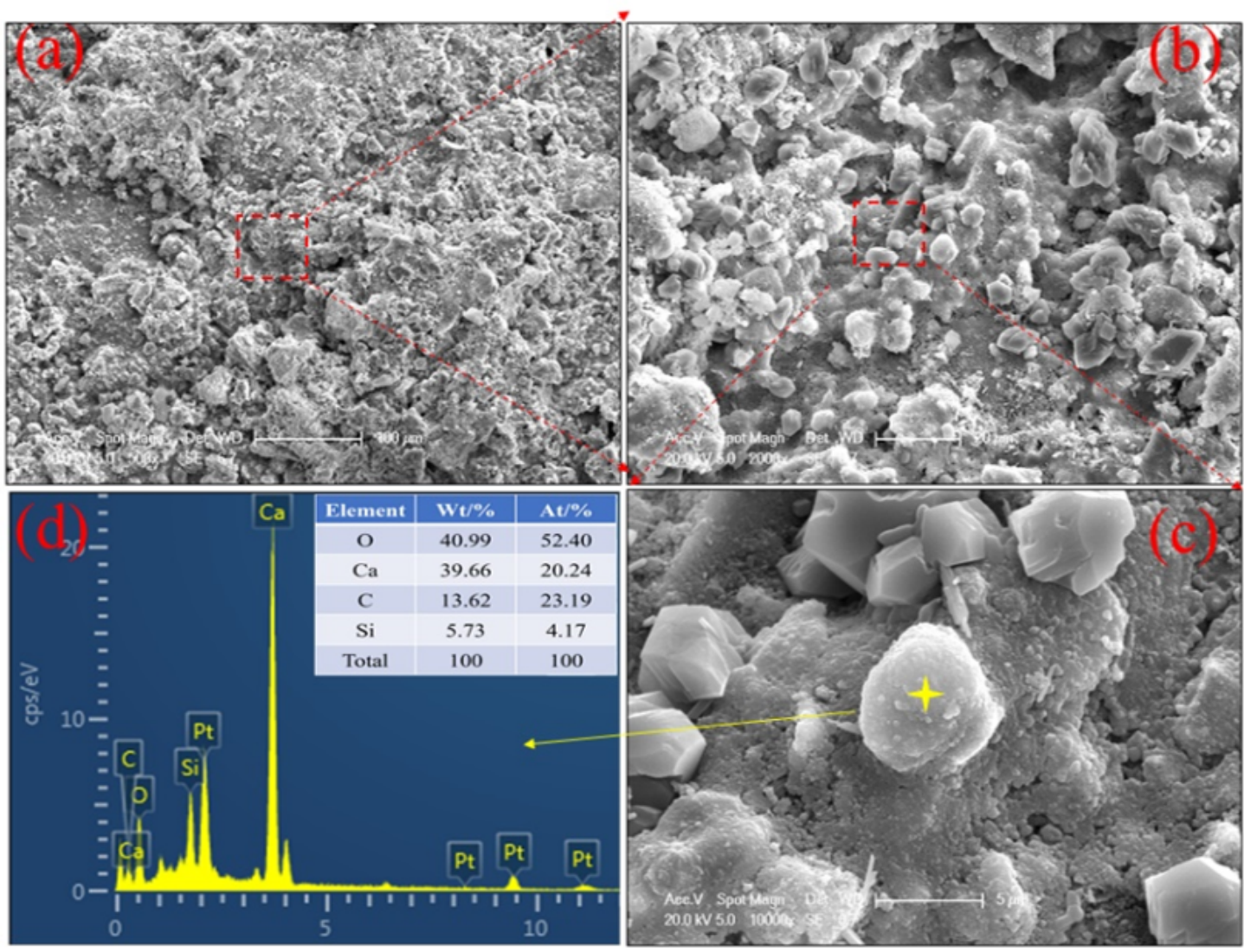


Figure 8

Porosity and pore size distribution of four-types artificial aggregate



**Figure 9**

SEM photographs of NB-C artificial aggregate: (a) 500-times magnification of specimen; (b) 2000-times magnification of red area; (c) 10000 times magnification of red area; (d) EDS analysis of yellow point in (c) graph

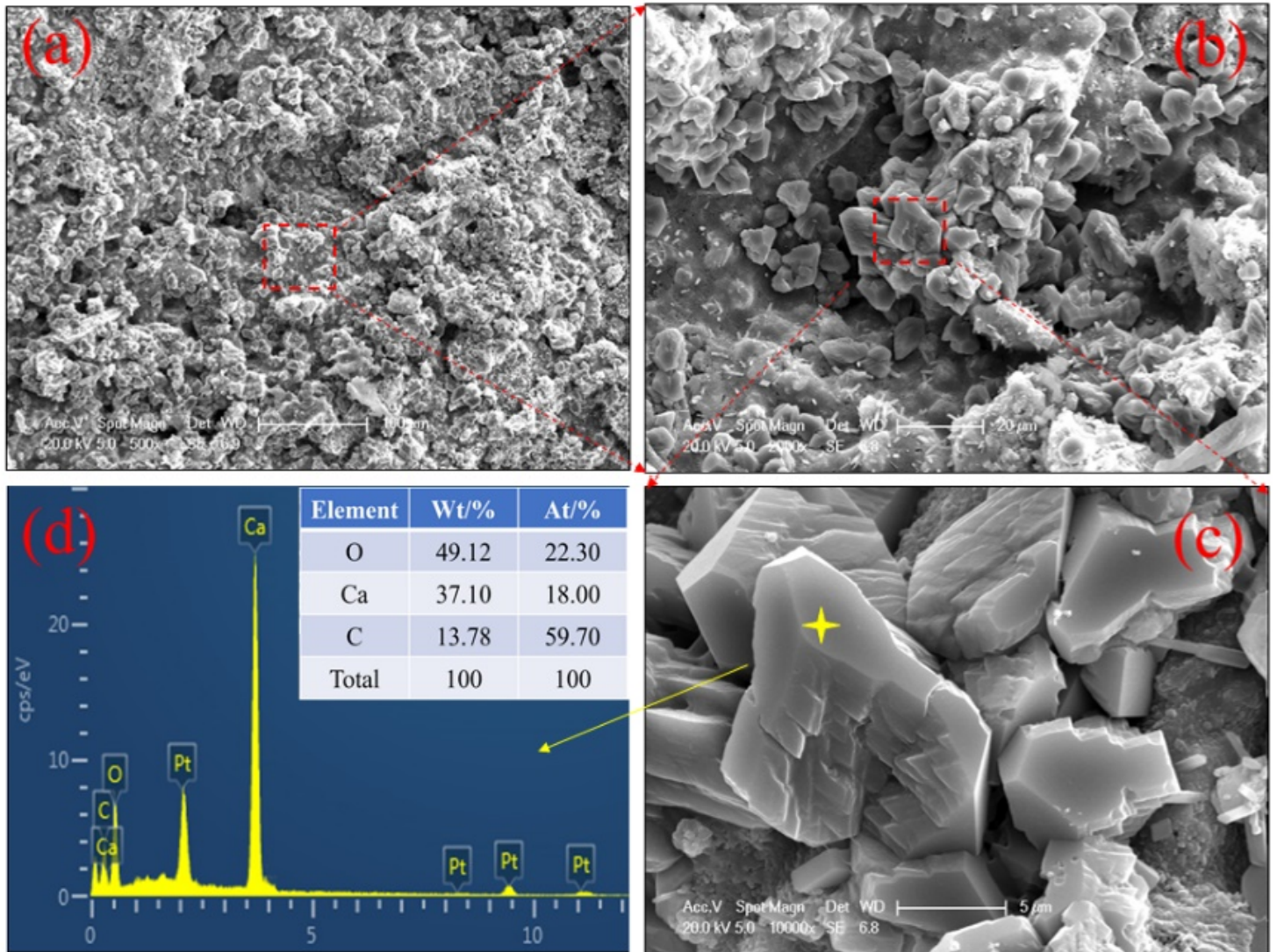


**Figure 10**

SEM photographs of B-C artificial aggregate: (a) 500-times magnification of specimen ; (b) 2000-times magnification of red area; (c) 10000 times magnification of red area; (d) EDS analysis of yellow point in (c) graph

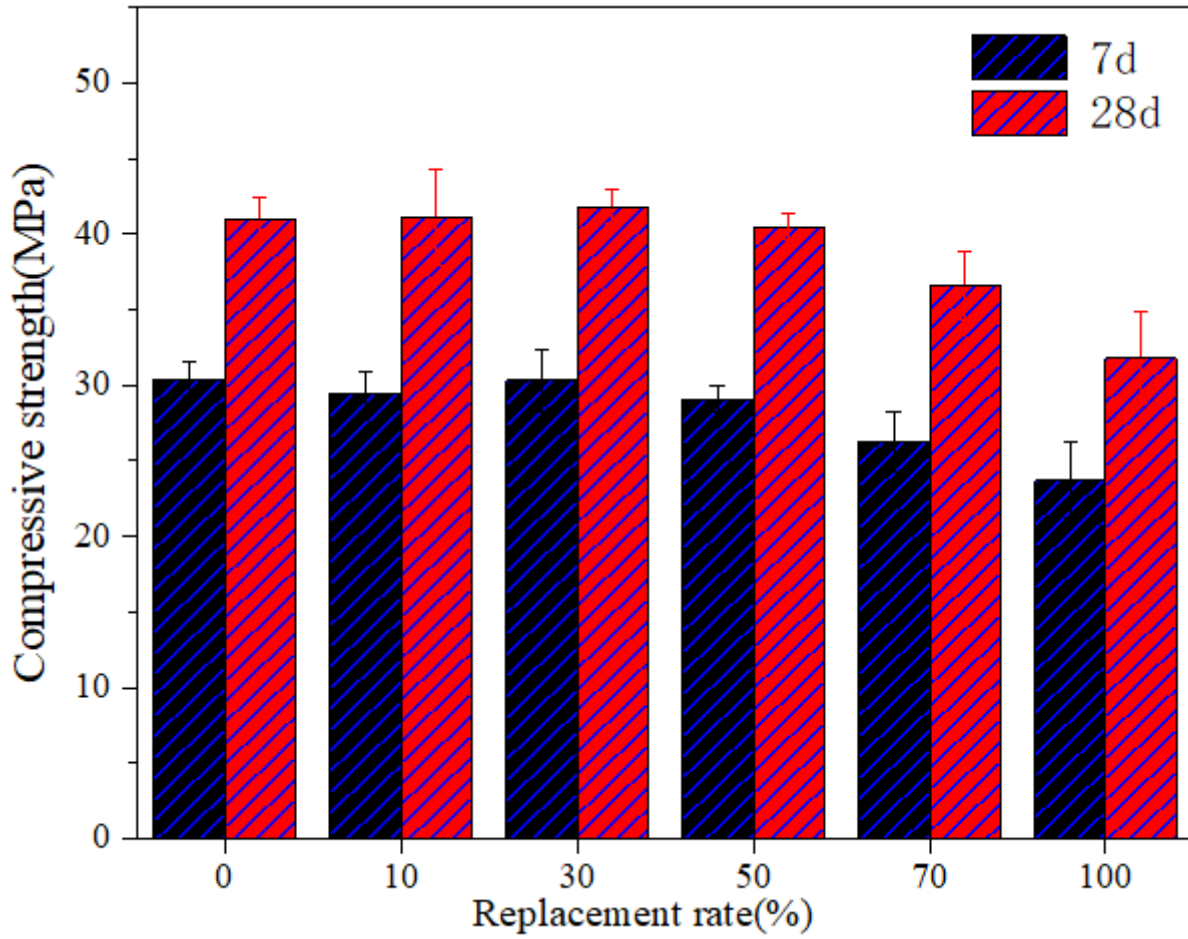


Figure 11

The compressive strength of concrete with different replacement ratios of artificial aggregate

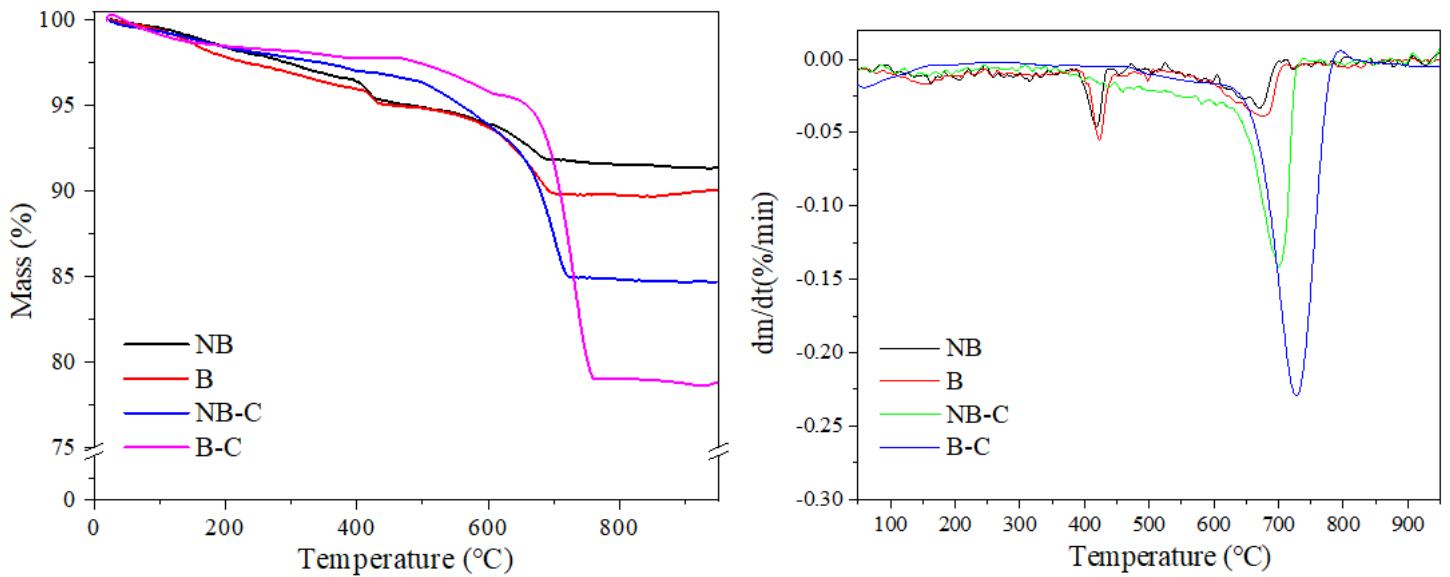


Figure 12

TG and DTG analysis of artificial aggregates

## Supplementary Files

This is a list of supplementary files associated with this preprint. Click to download.

- [GraphicalAbstract.docx](#)